Supplementary Information (SI) for New Journal of Chemistry.

Supporting Information

Waste-to-energy utilization by using PVDF-based flexible piezoelectric nanogenerator for efficient energy harvesting applications

Nil Lohit Sengupta, Suparna Ojha, Parna Maity, Sumanta Bera, Bhanu Bhusan Khatua*

Materials Science Centre, Indian Institute of Technology Kharagpur, Kharagpur -721302, India.

*Corresponding author

Prof. B. B. Khatua (Email: khatuabb@matsc.iitkgp.ac.in)

Materials Science Centre, Indian Institute of Technology Kharagpur, Kharagpur - 721302, India

Tel.: +91- 3222-283982

Flexibility checks of the composite

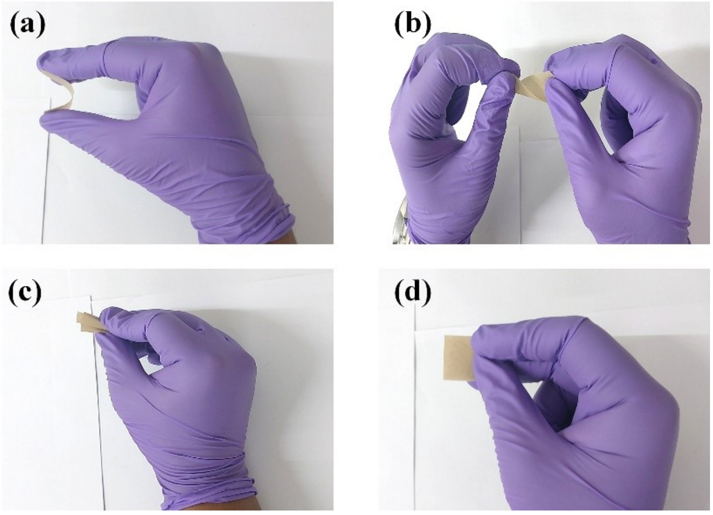

Figure S1: Flexibility check of the composite by (a) bending, (b) twisting, (c) rolling, (d) folding the composite.

FT-IR study

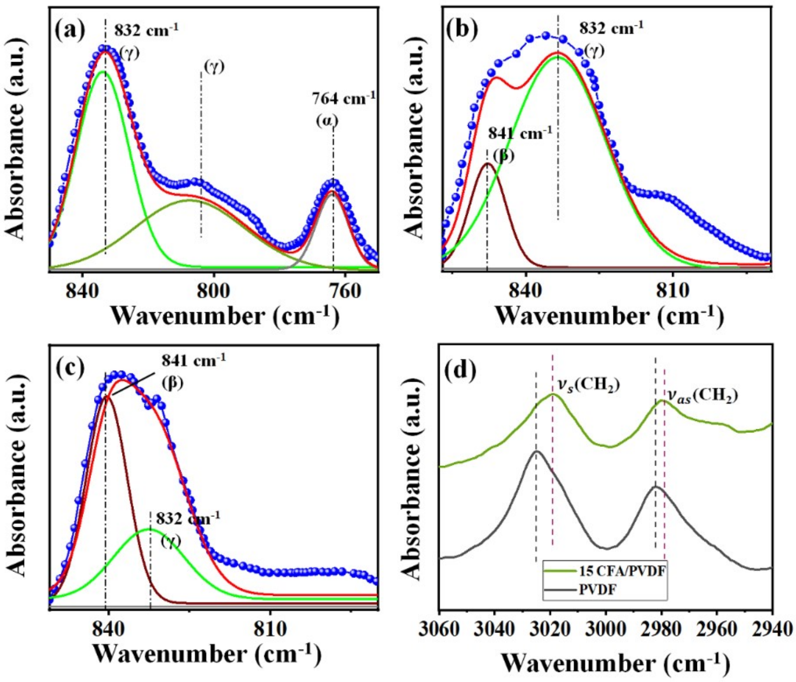

Figure S2: Deconvoluted FT-IR spectra of (a) pure PVDF, (b) 13 CFA/PVDF, (c) 15 CFA/PVDF composites. (d) FT-IR spectra of pure PVDF and 15 CFA/PVDF composite in the range of 2900-3100 cm^{-1}

From the deconvolution, a gradual increase of β phase can be observed in the PVDF composite with the increase in filler loading. The peak intensity at 832 cm^{-1} for the γ phase decreases and at 841 cm^{-1} for the β phase increases.

Table T1: Crystallinity by DSC study

CFA loading (%)	Melting temperature (T_m) (°C)	Crystalline Temperature (T_c) (°C)	Melting enthalpy ΔH_m (J/g)	Crystallinity (%)
0 %	160.0	130.69	37.7	36
10 %	160.52	131.49	40.08	42.6
13 %	160.92	132.18	41.1	45.2
15 %	161.51	132.77	47.4	53

The output performance, specifically in terms of piezoelectricity, of the composite is influenced by the degree of the polar crystalline phase, particularly the β-phase. Throughout the filler addition process, there is a progressive increase in the relative percentage of the β-phase in PVDF, with the maximum extent of the β-phase formation at a loading of 15 wt% of the CFA.

Zeta potential distribution of calcined fly ash (CFA)

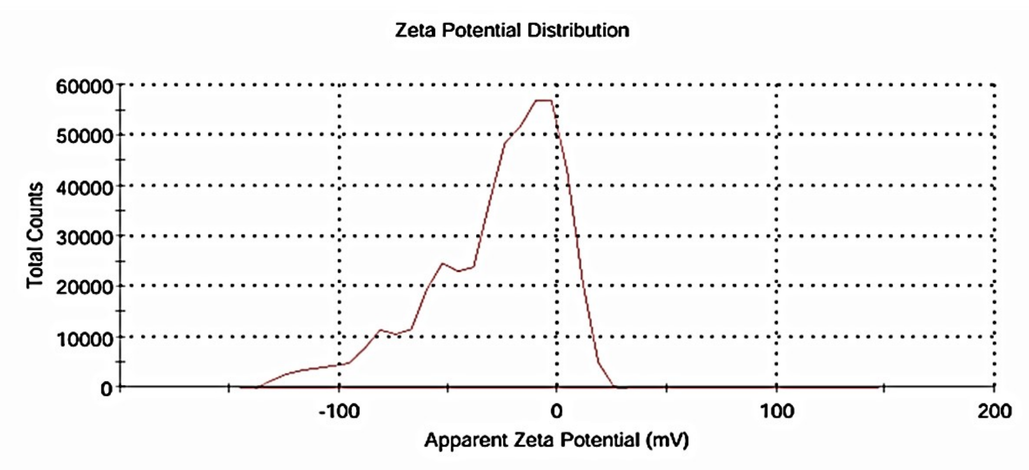

Figure S3: Zeta potential distribution of CFA

Working mechanism of WPNG

Previous discussions have indicated that the maximum extent of polar β phase is stabilised in the 15 CFA /PVDF composite as a result of the attractive interactions between the negatively charged surface of CFA particles and the $–CH_2–$ groups present in PVDF. Furthermore, the application of external force on the WPNG results in polarisation induced by stress[1]. In a neutral state, the dipole moment within the WPNG is null.

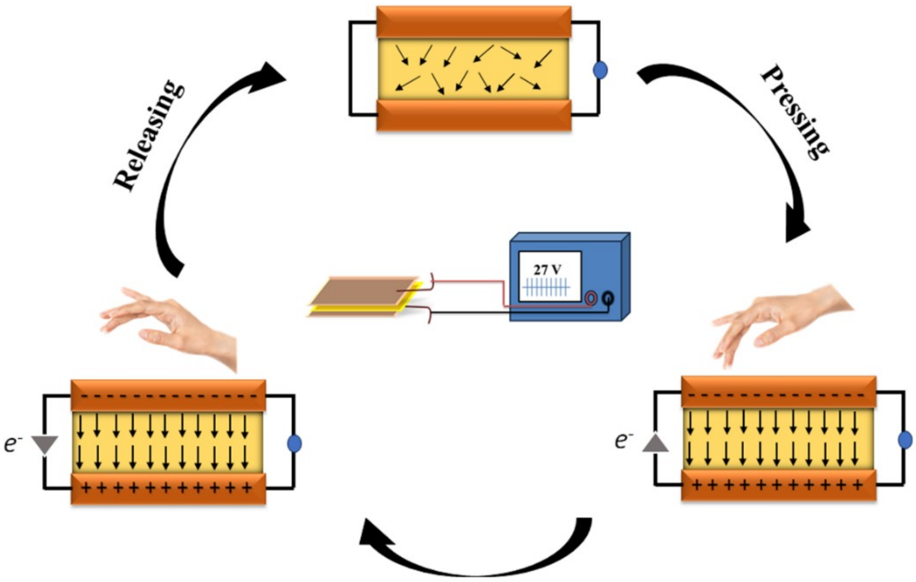

Figure S4: Working mechanism of WPNG

Upon the application of an external force on the WPNG, the dipoles exhibit a vertical alignment in a cohesive direction. As a result, contrasting charges accumulate on the surfaces of the WPEG, leading to the establishment of a potential difference. The observed potential difference facilitates the movement of electrons through the external circuit, as illustrated in the Figure S4. Upon removal of the pressure, a phenomenon known as electron backflow occurs. Output signals displayed on the oscilloscope illustrate the flow and backflow of electrons. Without any external pressure, the dipoles within the composite align randomly, leading to a net dipole moment of zero.

Calculation of applied pressure

Utilising a physical model that integrates the gravitational component with the pulse component, we have computed the pressure exerted by human fingers or a moving object on the WPNG. The process of an object falling on the WPNG device involves two distinct steps. Initially, the descending object makes contact with the surface of the apparatus. Secondly, the descending object exerts full pressure on the apparatus. In the initial process, the downward speed of the object in motion attains its peak value, whereas in the subsequent process, it diminishes to a value of zero. We can derive the following relationships grounded in the principles of kinetic energy and momentum conservation[2]:

$$m.g.h = \frac{1}{2}mv^2 \qquad \text{(S-1)}$$

$$(F - mg)\Delta t = mv \qquad \text{(S-2)}$$

$$\sigma = \frac{F}{S} \qquad \text{(S-3)}$$

Where m is the mass of the object, h is the height from where the pressure is applied, v is the maximum falling velocity, σ is the applied pressure or applied stress, F is the applied force, S is the active contact area of the device, and Δt is the time difference between two consecutive processes. Here S = 800 mm^2 electrode area of the MPNG. m = ~1kg as measured by using a laboratory balance, Δt = 0.25 sec, h = ~0.12 m and g = 9.8 N/kg. So, from the above values the calculated input force, F~16 N, gives the contact pressure, σ ~20 kPa.

Piezoelectric coefficient measurement

The piezoelectric coefficient of pure PVDF and CFA/PVDF composites was measured using a Piezotest PM300 machine, and the obtained data are presented in Table T2.

Table T2: Piezoelectric coefficient of pure PVDF and its composites

Materials	**Piezoelectric coefficient (d_{33}) [pC/N]**
Pure PVDF	4
10 CFA/PVDF	7
13 CFA/PVDF	9
15 CFA/PVDF	12

The piezoelectric values acquired from the Piezotest PM300 apparatus were subsequently cross-verified through frequency-dependent capacitance measurement (Figure S5). The measurement of capacitance as a function of frequency was conducted utilising an impedance analyser (Agilent 4294A, with a frequency range of 40 to 3×10^6 Hz), as illustrated in eq. S-4. Following this, the subsequent equation was employed to determine the piezoelectric coefficient.

$$V = \frac{F \times d_{33}}{C} \tag{S-4}$$

The output voltage of the PENG is represented as V, the applied force is indicated by F, the piezoelectric coefficient of the material is denoted by d_{33}, and the capacitance is represented by C.

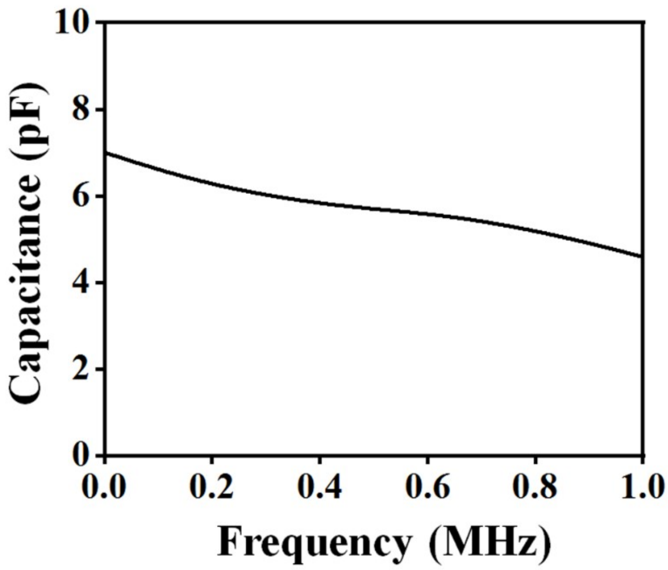

Figure S5: Capacitance vs. frequency curve of 15 CFA/PVDF composite

By applying the capacitance value C= 7 pF in Eq. S-4, the calculated piezoelectric coefficient (d_{33}) is approximately 12 pC/N, aligning closely with the d_{33} measurements acquired from the Piezotest PM300 machine.

Effect of external pressure

It is evident from Figure S6 that when the external pressure increases, the output voltage of the constructed PENG increases as well. When applying a pressure of around 20 kPa, the maximum voltage is approximately 27 V.

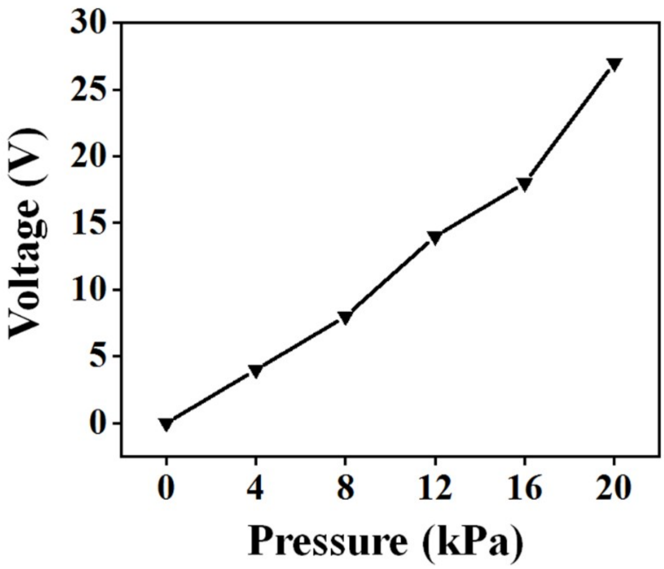

Figure S6: The variation in the generated voltage from the WPNG with the applied pressure

P-E hysteresis loop

Figure S7 illustrates the room temperature polarization-electric field hysteresis loops of pure PVDF and CFA/PVDF nanocomposites. Pure PVDF and CFA/PVDF nanocomposites underwent polarisation at a magnitude of 350 kV/cm and a frequency of 100 Hz. The image illustrates that the unmodified PVDF demonstrates a comparatively lower degree of polarisation when contrasted with the CFA/PVDF composites. The addition of filler leads to an increase in polarisation. The 15 CFA/PVDF exhibits the highest stabilisation of the β phase among all composites, resulting in a notable polarisation value. The predominant non-polar α-phase in pure PVDF leads to a significantly reduced area in the P-E hysteresis loop.

The increase in polarisation values of CFA/PVDF nanocomposites can be explained by the accumulation of charges at the interface between CFA particles and the PVDF chain.

The generation of charges fosters heterogeneous polarisation within the systems, consequently enhancing the ferroelectric properties of the sample[3].

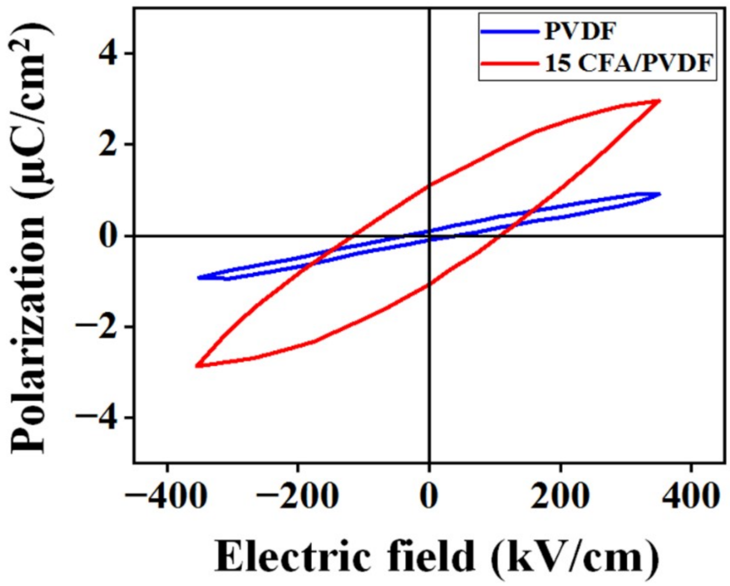

Figure S7: P-E hysteresis curve of pure PVDF and 15 CFA /PVDF nanocomposite.

The 15 CFA/PVDF nanocomposite exhibits a higher remnant polarisation (P_r = 1.05 μC/cm^2) compared to the pure PVDF film (P_r = 0.09 μC/cm^2). An increased P_r value enhances the 15 CFA/PVDF nanocomposite's effectiveness as a storage material. The 15 CFA/PVDF composite exhibits a spontaneous polarisation (P_s) of approximately 3 μC cm^{-2}, significantly surpassing that of pure PVDF. The spontaneous polarisation (P_s) and remnant polarisation (P_r) ratio is approximately 2.85 for the 15 CFA/PVDF composite, demonstrating well enough values at an electric field of around 350 kV/cm. This finding validates that the 15 CFA/PVDF composite demonstrates robust inherent piezoelectric characteristics.

Table T3: Comparison of fabricated nanogenerator (WPNG) with other reported PENG

Nanogenerator	Poling	Device area	Pressure/Force	Voltage(V)	Current(μA)
Fe-rGO/PVDF[4]	Not polled	6 cm^2	12 kPa	5.1	0.25
PVDF/rGO-MoS_2[5]	Not polled	-	15 kPa	2.4	0.68
PDA-$BaTiO_3$/PVDF[6]	Not polled	5.98 cm^2	12 N	9.3	0.08
BTO@HBP@PMMA/ PVDF[7]	polled	9 cm^2	40 N	3.4	0.32
rGO-Ag/PVDF[8]	Not polled	22 cm^2	4.6 kPa	18	1.05
PVDF/Mg-salt[9]	Not polled	7.2 cm^2	4.45 kPa	4	0.095
Coconut husk (CH)/ PVDF[10]	polled	2.89 cm^2	-	14 V	0.05
Fish scale/PVDF[11]	Not polled	0.49 cm^2	42 kPa	22 V	-
Bamboo micro particles/PVDF[12]	polled	6.25 cm^2	-	7.2 V	2.18
This Work	**Not polled**	**8 cm^2**	**20 kPa**	**27**	**0.3**

References

1. S. Bera, S. Ojha, P. Maity, N. L. Sengupta and B. B. Khatua, *Journal of Alloys and Compounds*, 2024, **1005**, 176038.
2. S. Ojha, S. Paria, S. K. Karan, S. K. Si, A. Maitra, A. K. Das, L. Halder, A. Bera, A. De and B. B. Khatua, *Nanoscale*, 2019, **11**, 22989-22999.
3. O. Jayakumar, E. H. Abdelhamid, V. Kotari, B. P. Mandal, R. Rao, V. M. Naik, R. Naik and A. Tyagi, *Dalton Transactions*, 2015, **44**, 15872-15881.
4. S. K. Karan, D. Mandal and B. B. Khatua, *Nanoscale*, 2015, **7**, 10655-10666.
5. M. Faraz, H. H. Singh and N. Khare, *Journal of Alloys and Compounds*, 2022, **890**, 161840.
6. Y. Yang, H. Pan, G. Xie, Y. Jiang, C. Chen, Y. Su, Y. Wang and H. Tai, *Sensors and Actuators A: Physical*, 2020, **301**, 111789.
7. B. Zhao, Z. Chen, Z. Cheng, S. Wang, T. Yu, W. Yang and Y. Li, *ACS Applied Nano Materials*, 2022, **5**, 8417-8428.
8. M. Pusty, L. Sinha and P. M. Shirage, *New Journal of Chemistry*, 2019, **43**, 284-294.
9. S. Jana, S. Garain, S. Sen and D. Mandal, *Physical Chemistry Chemical Physics*, 2015, **17**, 17429-17436.
10. M. Sahu, S. Hajra, S. Jadhav, B. K. Panigrahi, D. Dubal and H. J. Kim, *Sustainable Materials and Technologies*, 2022, **32**, e00396.
11. C. Kumar, A. Gaur, S. Tiwari, A. Biswas, S. K. Rai and P. Maiti, *Composites Communications*, 2019, **11**, 56-61.
12. N. D. Kulkarni, A. Saha and P. Kumari, *Journal of Applied Polymer Science*, 2023, **140**, e54040.